A contribution to the deterministic modelling of circadian rhythms in cell proliferation activity

M. Nieto

Junta de Energía Nuclear, Avda. Complutense, 22-Madrid, Spain

R. Alvarez, M. A. Hacar and E. Alarcon

Universidad Politécnica, Madrid

This paper presents a deterministic continuous model of proliferative cell activity. The classical series of connected compartments is revisited along with a simple mathematical treatment of two hypotheses: constant transit times and harmonic T_s. Several examples are presented to support these ideas, both taken from previous literature and recent experiences with the fish *Carassius auratus*, developed at the Junta de Energía Nuclear, Madrid, Spain.

Keywords: mathematical model, circadian rhythm, proliferation activity, transit times, fraction labelled mitosis

Circadian rhythms may be considered as those biological rhythms which, under constant and permissive conditions, continue to exhibit oscillations with a period of about (*circa* one day (*diem*). The circadian rhythm, is synchronized with, or entrained to, the period of the earth's rotation by means of periodic factors in the environment, called Zeitgebers. The day–night changes in illumination and temperature are the most important of these. The light–dark (LD), cycle does not cause the rhythms, they are innate and endogenous. Under different permissive environmental conditions (light intensity, temperature), the period is conserved within relatively narrow limits.

The induction of a circadian oscillation by an entraining LD cycle exerts control over both the period and the phase of the endogenous rhythm. In the dark–dark (DD) cycle (constant darkness) the rhythm will persist, be free running, and expressing its innate period.

Chronobiology has become particularly important as a result of the synchronization of experimental animals to an artificial light–dark cycle in order to design and interpret the experimental results. Living organisms are not uniform or stable in their normal body states; instead, an organism is different at different circadian stages and, therefore, reacts differently to an identical stimulus during the day. For instance, an identical dose of drugs has dramatically different effects at various times of the day.

There are many circumstances in which it is interesting to relate circadian rhythms to the effects of a drug dose in a biological process. In this paper, the authors concentrate on the way in which cells increase their number in the intestine of goldfish, although other cases previously treated in the literature are also commented upon.

It is generally accepted that cells reproduce through a cycle with four stages called G_1, S, G_2 and M. M stands for mitosis, i.e. the phase in which the chromosomes become visible and cell division occurs, S for dexosiribonucleic acid (DNA) synthesis, and G_1 and G_2 are gaps during which no DNA synthesis occurs, although RNA and protein synthesis occurs throughout both gaps and the S phase. The cell spends different times T_1, T_2, T_3 and T_4 in each phase (though the shortest one is mitosis), and the cycle duration is $T_c = T_1 + T_2 + T_3 + T_4$, at the end of which the cell has duplicated.

Table 1 Average cell fluxes over 24 h in partially synchronized renewing cell systems at different cell cycle phases: experimental results (percentage of cells per hour)

Integral average/ transit time	$\bar{N}_4/T_4$	$\bar{N}_2/T_2$	$\bar{N}_4/T_4$	$\bar{N}_2/T_2$	Observations
Brown and Berry[18]	0.63/1.0 0.63	5.25/ 8.6 0.61	0.63/1.2* 0.53	5.25/9.9 0.53	* From Hopper and Brokwell[28]
Izquierdo and Gibbs[17]	0.50/0.95 0.53	4.08/ 9.0 0.45	0.50/1.2* 0.42	4.08/9.9* 0.41	
Izquierdo and Gibbs[16]	1.08/0.98 1.11	9.38/ 8.0 1.17	1.08/1.2* 0.90	9.38/9.9* 0.95	
Hegazy and Fowler[15]	1.2 /1.4 0.86	10.7 /11.5 0.93	— —	— —	Unplucked
	2.2 /1.2 1.83	22.5 /10.7 2.10	— —	— —	Plucked
Carassius auratus at 25°C	0.41/0.77 0.53	8.0 /15.0 0.53	— —	— —	Cells per hour per fold section
Clausen *et al.*[19]	1.82/1.0 1.82	16.83/ 8.8 1.91	6.0/3.2† 1.81	— —	† Percentage of cells with G_2 DNA (means corrected for GF = 0.60)

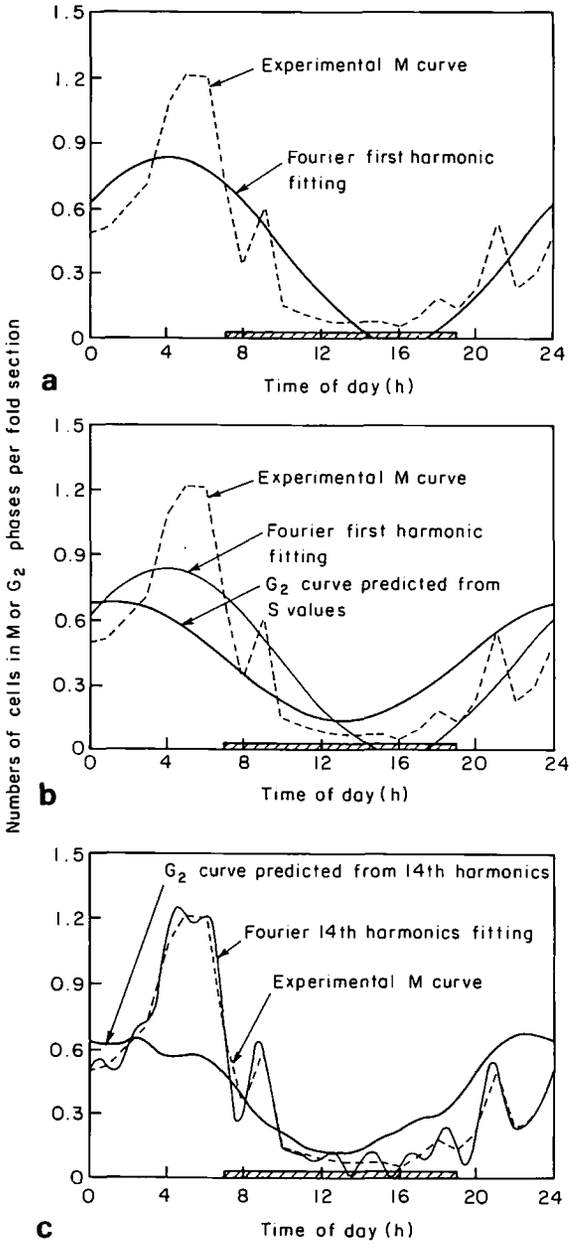

Figure 1 Goldfish intestine: shading indicates period of darkness

Table 2 Number of cells per fold section in DNA synthesis, N_2, and in M phase, N_4 of goldfish intestine

Time of day (h)	$N_2 \pm ES$		$N_4 \pm ES$	
00.00	10.82	1.82	0.51	0.12
01.00	13.72	3.88	0.52	0.13
02.00	13.24	2.39	0.61	0.13
03.00	7.07	2.55	0.71	0.17
04.00	11.72	2.34	1.08	0.25
05.00	10.53	1.09	1.22	0.39
06.00	7.31	2.37	1.21	0.26
07.00	2.55	0.80	0.67	0.11
08.00	1.07	—	0.34	—
09.00	2.45	1.81	0.61	0.18
10.00	0.85	0.16	0.15	0.13
11.00	0.99	0.14	0.11	0.10
12.00	3.24	1.47	0.09	0.03
13.00	2.54	0.97	0.07	0.03
14.00	5.47	2.71	0.07	0.03
15.00	5.84	1.54	0.08	0.03
16.00	7.22	1.61	0.05	0.03
17.00	6.48	1.75	0.10	0.09
18.00	9.58	2.87	0.19	0.07
19.00	14.03	1.89	0.13	0.05
20.00	15.94	3.03	0.23	0.11
21.00	15.09	3.45	0.53	0.27
22.00	12.47	1.25	0.23	0.08
23.00	11.44	2.45	0.30	0.10
24.00	10.82	1.82	0.51	0.12

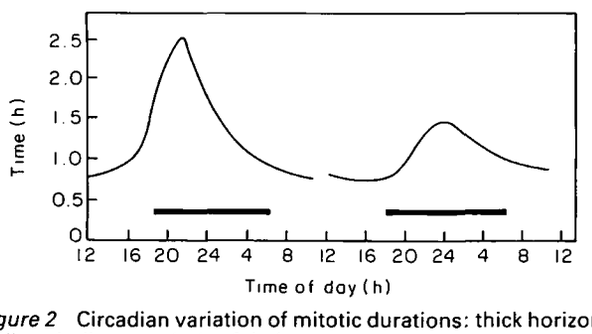

Figure 2 Circadian variation of mitotic durations: thick horizontal lines indicate periods of darkness

Table 3 Mitotic and labelling indices in hamster cheek pouch epithelium[16]

Time of day (h)	N_4	N_S
02.00	0.006 ± 0.002	0.08 ± 0.03
04.00	0.007 ± 0.003	0.14 ± 0.01
06.00	0.009 ± 0.001	0.15 ± 0.01
08.00	0.010 ± 0.004	0.15 ± 0.01
10.00	0.022 ± 0.001	0.15 ± 0.01
12.00	0.024 ± 0.001	0.12 ± 0.01
14.00	0.015 ± 0.003	0.09 ± 0.01
16.00	0.016 ± 0.001	0.06 ± 0.01
18.00	0.016 ± 0.003	0.04 ± 0.01
20.00	0.008 ± 0.001	0.03 ± 0.01
22.00	0.005 ± 0.002	0.04 ± 0.01
24.00	0.002 ± 0.001	0.08 ± 0.01

Table 4 Variables of epidermal basal cells in hairless mouse epidermis[19]

Time of day (h)	Cells with S-phase DNA content (%)	Cells with G_2-phase DNA content (%)	N_4 (%)
00.00	13.67	6.83	2.18
02.00	16.17	5.17	1.87
04.00	15.33	4.83	2.07
06.00	15.00	4.83	0.75
08.00	15.17	4.33	1.12
10.00	20.17	8.67	1.47
12.00	26.67	6.00	1.87
14.00	23.67	6.17	1.50
16.00	22.33	7.33	1.33
18.00	20.50	7.00	5.22
20.00	15.17	7.50	2.53
22.00	14.50	6.50	2.33
24.00	13.67	6.83	2.18

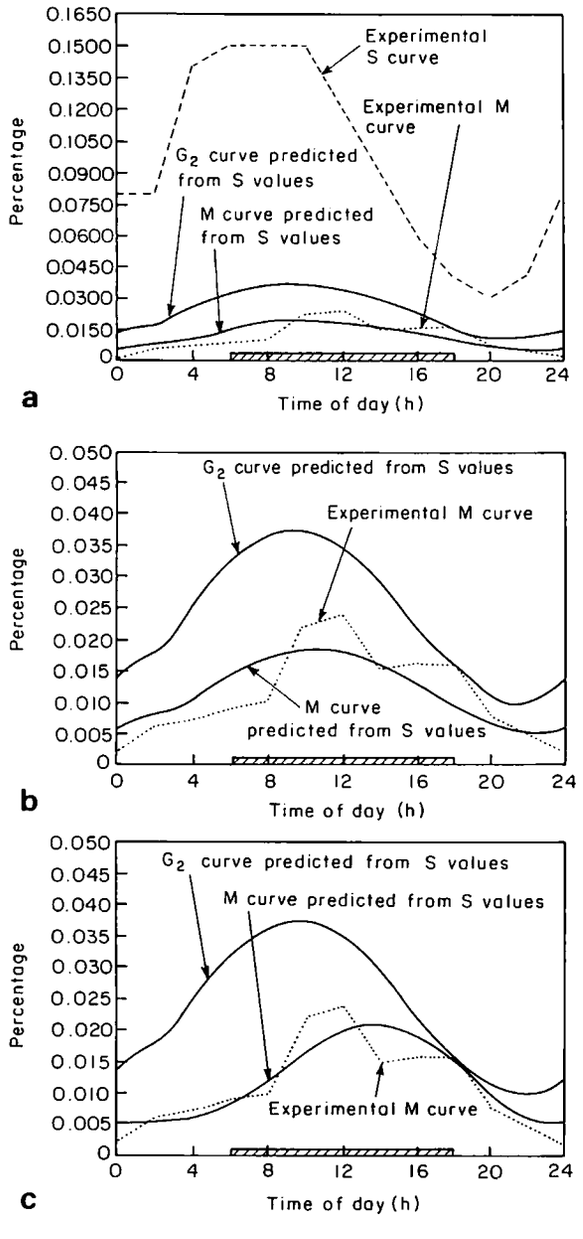

Figure 3 Hamster pouch:[16] shading indicates periods of darkness

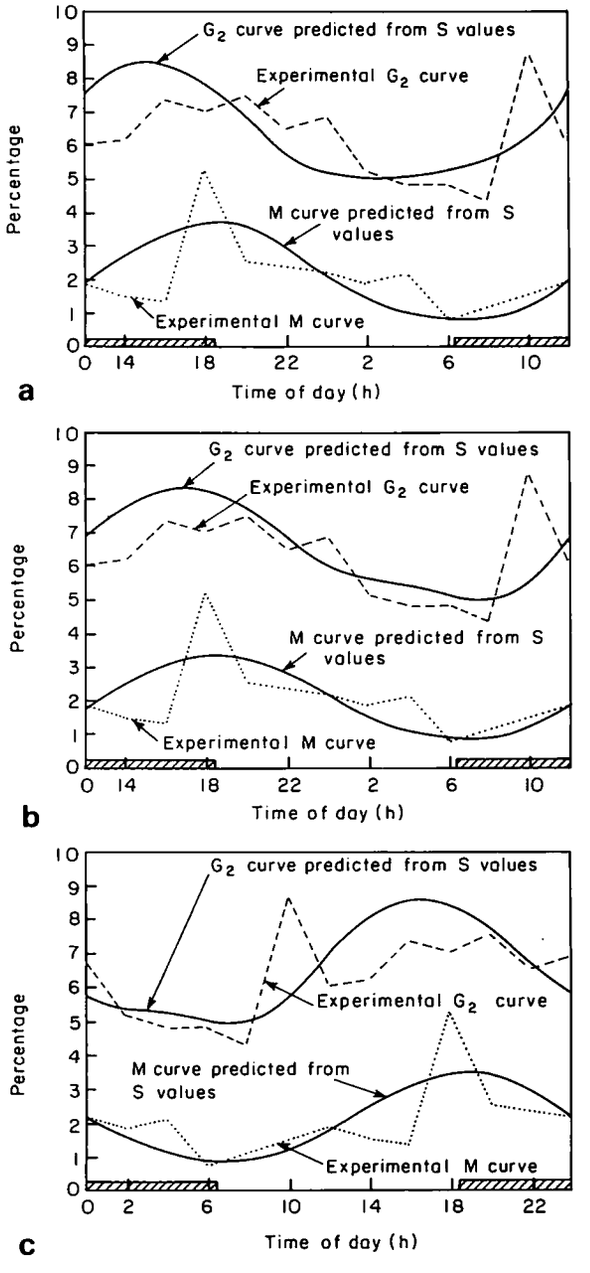

Figure 4 Mouse epidermal basal cells:[19] shading indicates period of darkness

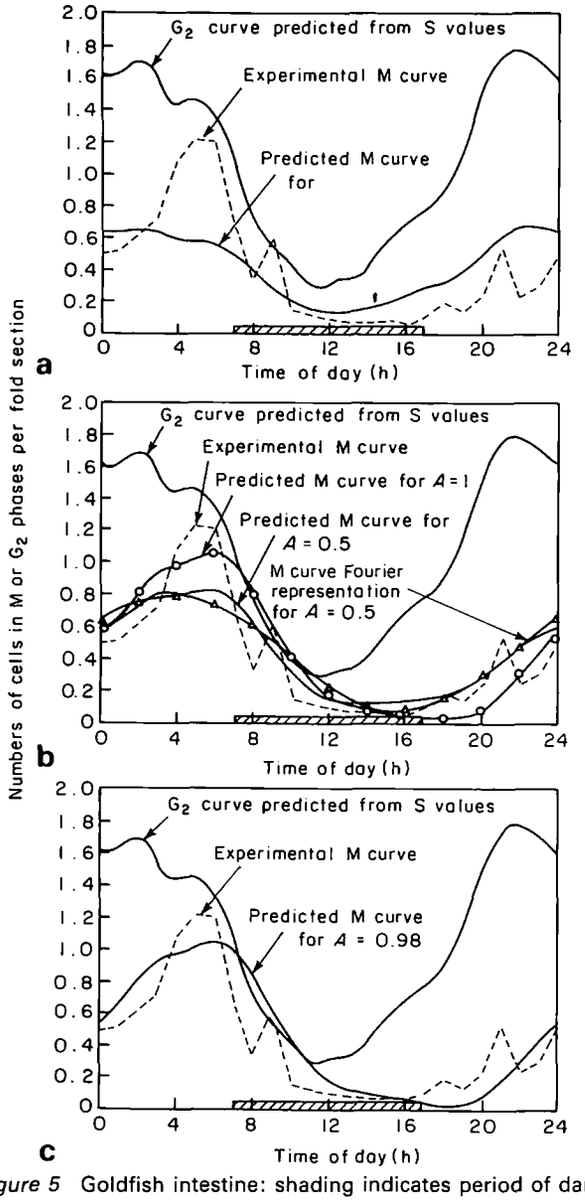

Figure 5 Goldfish intestine: shading indicates period of darkness

When cells in proliferation are briefly exposed to ^{3}HTdr, deoxyribonucleoside thymine, the radiative precursor of DNA, incorporation follows and affected cells are classified as labelled cells in autoradiography. The other phases may be separated according to their DNA content. The DNA content of G_2 cells, corresponding to cells in which DNA replication has been completed, is double that of G_1 cells in which DNA replication has not yet begun.

It is assumed that cells are involved in the continuous cycle of replication and cell division. This is true for most cases in tissue cultures, but in most body tissues only a fraction of the total cell population is involved in this cycle and the remainder are involved in other functions. The fraction of the population involved in the cell cycle is defined as the growth fraction. The analysis of the problem was initially approached by assuming that the number of cells in each phase was constant throughout the process; i.e. a rectangular distribution was assumed.

But not all of the renewing cellular systems can be described by a rectangular distribution implying the existence of steady state growth kinetics with a constant frequency distribution of cells throughout the mitotic cycle.[1–6] Many results, however, have clearly shown that these systems exhibit a circadian rhythm in mitotic and DNA synthesis activity.[7–23]

Izquierdo and Gibbs,[17] in order to avoid the influence of circadian variations on the proliferation rate, introduced the numerical integration of the circadian mitotic curve. The proliferation rate (PR) was defined as the fraction of the cell population that has completed mitosis in a time unit. Under circadian fluctuation, this time unit should be 24 h as equations based on total asynchrony cannot be used.

The reciprocal of the proliferation rate:

$$TT \cong 1/PR \tag{1}$$

is called turnover time TT.

As a definition of PR, Izquierdo and Gibbs used the expression:

$$PR = \int_0^{24} N_4(t)\mathrm{d}t \tag{2}$$

where $N_4(t)$ is the number of cells in the mitotic phase at time t, although the correct definition should be:

$$PR = \frac{1}{T_4}\int_0^{24} N_4(t)\mathrm{d}t \tag{3}$$

The use of repeated injections of ^{3}H-Tdr allowed them to measure an approximate turnover time of nine days, in good agreement with the value given by equation (1), 8.4 days for the Syrian hamster. Similar agreement is obtained with the Chinese hamster, 3.8 and 4.0 days, respectively.

The coincidence between the measured turnover time and that obtained from expression (2), is due to the fact that T_4 is almost equal to one. For instance, T_4 measured by Izquierdo and Gibbs[17] in the Syrian hamster cheek pouch epithelium was 0.95 ± 0.16 h and they found a T_4 value of 0.98 ± 0.16 h for the Chinese hamster.[16]

The usefulness of definition (3) lies in the experimental fact that, if all of the cells that go through the S phase complete mitosis,[5,6,24] the numerical integration of the number of cells in synthesis N_2 divided by T_2 gives the same flux PR, i.e.:

$$PR = \int_0^{24} (N_2\mathrm{d}t/T_2) \tag{4}$$

The proliferation rates computed from expression (3) and (4) are shown in *Table 1*, for different cell renewing systems.

The circadian variations of T_4 have been measured by Burns and Scheving[25] in the mouse corneal epithelium twice a day at 09.00 and 21.00 h. The measured T_4 were 12.2 and 5.4 h, respectively. In the cheek pouch epithelium of a Syrian hamster, Moller *et al.*, found a T_4 of 8.0–13.5 h.[26] This is comparable with the circadian variation of T_4 in mouse epidermis of 5.2–12.5 h found by Tbermyr.[27] Izquierdo and Gibbs,[17] working at two times of the day, 08.00 a.m. and 08.00 p.m. obtained approximately 9.0 h for the cheek pouch epithelium in the Syrian hamster. The same authors[16]

obtained a T_2 of 8.0 h in the Chinese hamster. Hopper and Brockwell[28] have developed a stochastic model and computed the expected values for T_2 in the Syrian hamster cheek pouch epithelium; T_2 varies between 7.8 and 11.7 h, with an average of 9.9 h. The same authors[24] computer a T_4 of 1.20 h, and suggest that one should measure three or more fraction labelled mitosis curves in order to obtain a better value of T_2. Sternfeld[20] found a T_2 of 14.3 and 14.8 h for the intestinal epithelium of the common goldfish (*arassius auratus*), acclimated at 25°C, twice a day, for maximum and minimum values of the number of cells in the S phase per fold section. Unpublished data gives a T_2 of 16.52 h for the same conditions specified.

In the presence of circadian rhythms, the distribution of cells in mitosis or synthesis depends on the time of day, and also the time taken by a cell to pass through any phase; as a consequence of this, the cell flux is also time-dependent.

The proliferation rate for a steady state growth with asynchronous proliferation activity is:

$$(N_4/T_4) = (N_2/T_2) \tag{5}$$

The influence of partial synchronization of the parameters can be avoided using the integral average, on 24 h:

$$(\bar{N}_2/T_2) = (\bar{N}_4/T_4) \tag{6}$$

Geometrically the integral average is equivalent to a rectangle with a base equal to the period, 24 h, and height equal to the average value of the parameter during 24 h.

Table 1 shows the values calculated for different renewing cells systems. As a consequence, the mean phase durations can be directly calculated by converting the proportions of cells in each phase to the corresponding percentage of T_c, assuming a steady state of growth.[19]

The aim of this paper is the fitting of the circadian proliferation curves in renewing cells systems that are partially synchronized using a deterministic mathematical model. In the fitting of the curves two conditions are specified, firstly that the transit times, T_3 and T_4, are constant during the day and, secondly, that T_4 varies with time during the day.

Mathematical model

The mathematical modelling of the processes described has reached a considerable degree of sophistication.[29] In general, good agreement can be obtained through refined probabilistic continuous models. Nevertheless, the point is that it seems worthwhile to reattempt a continuous deterministic approach based on mean values or to change the techniques used for classifying the input data following modern, statistical trends.

This paper will develop the first topic. The above-mentioned facts suggest the use of a series of deposits of cells, the first of which is entered by a stream $Q(t)$ that can be seen as originating from recycling cells.

The first idea is to assume constant transit times and that the flux variation is directly proportional to the numbers of cells and inversely proportional to the transit time. If N_j is the number of cells (absolute or relative) in each phase, the equations of the continuous model can be written as:

$$\dot{N}_1 = Q - \frac{N_1}{T_1}$$

$$\dot{N}_j = \frac{N_{j-1}}{T_{j-1}} = \frac{N_j}{T_j} \quad (j = 2, 3, 4) \tag{7}$$

where the correspondence among indexes and phases is:

gap 1	T_1
DNA synthesis	T_2
gap 2	T_3
mitosis	T_4

(8)

and T_i are the transit times for every phase.

The properties of the system are:

(1) If a period T exists, integration of equation (1) yields:

$$\int_0^T Q\mathrm{d}t = \int_0^T \frac{N_1\mathrm{d}t}{T_1}$$

$$\int_0^T \frac{N_{j-1}\mathrm{d}t}{T_{j-1}} = \int_0^T \frac{N_j\mathrm{d}t}{T_j} \qquad j = 2, 3, 4 \tag{9}$$

If transit times are constant:

$$\int_0^T Q\mathrm{d}t = \frac{1}{T_1}\int_0^T N_1\mathrm{d}t = \frac{1}{T_2}\int_0^T N_2\mathrm{d}t$$

$$= \frac{1}{T_3}\int_0^T N_3\mathrm{d}t = \frac{1}{T_4}\int_0^T N_4\mathrm{d}t \tag{10}$$

(2) Dividing by the common period, equation (10) can be written as:

$$\frac{1}{T}\int_0^T Q\mathrm{d}t = \frac{1}{T_1}\left(\int_0^T N_1\mathrm{d}t/T\right)$$

$$= \frac{1}{T_2}\left(\int_0^T N_2\mathrm{d}t/T\right) = \frac{1}{T_3}\left(\int_0^T N_3\mathrm{d}t/T\right)$$

$$= \frac{1}{T_4}\left(\int_0^T N_4\mathrm{d}t/T\right)$$

giving a mathematical expression to the facts previously described.

(3) The extreme left-hand side of equation (11) is the mean value of $Q(t)$ and equals the mean values at each phase multiplied by the reciprocal of the appropriate transit time.

(4) Adding numerators and denominators in equation (11):

$$\bar{Q} = \frac{1}{T_C}\left(\int_0^T N_{TOT}\mathrm{d}t/T\right)$$

$$\bar{Q} = \frac{\bar{N}_{TOT}}{T_C} \tag{12}$$

where N_{TOT} is the total number of cells; T_C the cycle time; $\bar{N}_{TOT}$ the mean value of N_{TOT}; and $\bar{Q}$ the mean value of Q. In other words, the mean value of $Q(t)$ is equal to the mean value of the total number of cells divided by the cycle time.

The solution of the model is immediate and can be separated into stationary and harmonic responses. The first is obtained when:

$$Q(t) = Q_o(t) = \text{constant} \tag{13}$$

Evidently:

$$\dot{N}_1 = \dot{N}_2 = \dot{N}_3 = \dot{N}_4 = 0 \tag{14}$$

$$Q_o = \frac{N_1}{T_1} = \frac{N_2}{T_2} = \frac{N_3}{T_3} = \frac{N_4}{T_4} \tag{15}$$

Equation (15) is a particular case of equation (11) and produces the first approach to the solution:

$$N_j = T_j Q_o \qquad j = 1, 2, 3, 4$$
$$N_{TOT} = T_C Q_o \tag{16}$$

The harmonic response is obtained when:

$$Q = Q_n \exp(i\omega_n t) \tag{17}$$

and putting:

$$N_1 = A_1 \exp(i\omega_n t) \tag{18}$$

in the first of equations (1):

$$A_1/T_1 = Q_n/(1 + 1\omega_n T_1) \tag{19}$$

Similarly:

$$A_2/T_2 = Q_n/[(1 + i\omega_n T_1)(1 + i\omega_n T_2)]$$
$$A_3/T_3 = Q_n/[(1 + i\omega_n T_1)(1 + i\omega_n T_2)(1 + i\omega_n T_3)]$$
$$A_4/T_4 = Q_n/[(1 + i\omega_n T_1)(1 + i\omega_n T_2)$$
$$(1 + i\omega_n T_3)(1 + i\omega_n T_4)] \tag{20}$$

That is, the transit through a phase j is characterized by a transfer function:

$$H(\omega) = 1/(1 + i\omega_n T_j) \tag{21}$$

It is possible, of course, to treat equation (20) by separating modules and phases:

$$N_j/T_j = Q_n/\left\{\prod_{i=1}^{j} [1 + 4\pi^2(T_i^2/T_n^2)]\right\}$$
$$\exp\left\{[(2\pi/T_n)] - \sum_{i=1}^{j} \tan^{-1}[(2\pi(T_i/T_n)]\right\} \tag{22}$$

where:

$$\omega_n = (2\pi/T_n)$$

Due to the linear properties of the systems it is possible to analyse the case:

$$Q = Q_o + \sum_{n=1} Q_n \exp(i\omega_n t) \tag{23}$$

by superimposing the previous solutions:

$$N_j/T_j = Q_o + \sum_{n=1}^{N}$$
$$\left\{Q_n/\prod_{i=1}^{j}(1 + i\omega_n T_i)]\right\}\exp(i\omega_n t) \tag{24}$$

$$N_j/T_j = Q_o + \sum_{n=1}^{N}$$
$$\left(Q_n/\prod_{i=1}^{j} [1 + 4\pi^2(T_i^2/T_n^2)]\right.$$
$$\left.\exp\left\{\left[(2\pi/T_n) - \sum_{i=1}^{j} \tan^{-1}(2\pi(T_i/T_n)\right]\right\}\right) \tag{25}$$

The simple representation of the transfer function in the frequency domain and its linearity, allows the prediction of any of the curves $N_i(t)$ as soon as one is developed as a Fourier series of the type:

$$N_i = N_i^0 = \Sigma N_i^n \exp(i\omega_n t) \tag{26}$$

The system behaves as a series of filters. When coming down from the G_1 to the M phase (downwind), they smooth the noise of the data, while sharpening the curvature when proceeding in the reverse direction (upwind). In order to show clearly what is happening, the experimental data is not subjected to any kind of smoothing technique.

The authors, however, have developed the experimental data as a Fourier series, which means that the higher harmonics are actually noise which will disappear in downwind predictions, but will completely pollute the response in upwind ones.

As an example, *Figure 1(a)* represents the measured M numbers and the constant plus fundamental tone of its Fourier development, for the case represented in *Table 2*. *Figure 1(b)* presents a comparison with the prediction from data of the synthesis phase and *Figure 1(c)* shows the series development of the M phase and the predicted response when treating the full Fourier series development of the S phase and transmitting it through the model.

The transit times taken for that example were:

$$T_2 = 15.0\,\text{h} \qquad T_3 = 2.0\,\text{h} \qquad T_4 = 0.77\,\text{h}$$

As can be seen in *Figure 1(b)*, the prediction is not entirely satisfactory due to:

(a) a phase shift of about 2 h between the data and the prediction
(b) a difference in amplitude of about 30%

Both effects were also noticed when running other published data. Nevertheless, the adjustment for predicted G_2 results, when starting with S data, was observed to be relatively good and, in all cases, the mean value equality of equation (11) was rigorously satisfied.

In order to improve the results the authors tried to vary the estimated transit times without any noticeable variation of the mean trends (shown). *Figure 2*, taken from Clausen *et al.*,[19] suggests that the evolution of mitotic transit times, T_4, follows a periodic shape that is simulated here by a harmonic curve. That implies the use of field equations of the type described previously but with periodic coefficients in place of the previously-assumed constant transit times.

In order to reduce the parameters and because of the numerical experiences with other results, it was decided to make just time T_4 periodic, i.e. it was assumed that only the mitotic transit time varies with the hour and that it follows an evolution of the type:

$$T_4 = \bar{T}_4 + A \sin[(2\pi x/24) - \phi]$$

where $\bar{T}_4$ is the mean value, A is the relative amplitude and ϕ the time phase shift with respect to hour zero. The

model described is only valid for the first three numbers, N_1, N_2 and N_3, while the fourth must be calculated following another technique.

Due to the reduced dimensions of the problem, the use of a step-by-step method based on very small time steps does not represent a handicap of the total computational time. This allows the use of a simple Euler method to substitute the derivative according to the simplest formula:

$$\Delta_t y(t) = y(t + \Delta t) - y(t) \tag{27}$$

where Δt is adjusted in order to guarantee the stability and convergence of the procedure.

Set (7) can be written as:

$$\begin{bmatrix} \dot{N}_1 \\ \dot{N}_2 \\ \dot{N}_3 \\ \dot{N}_4 \end{bmatrix} = \begin{bmatrix} -\frac{1}{T_1} & 0 & 0 & 0 \\ \frac{1}{T_1} & -\frac{1}{T_2} & 0 & 0 \\ 0 & \frac{1}{T_2} & -\frac{1}{T_3} & 0 \\ 0 & 0 & \frac{1}{T_3} & -\frac{1}{T_2} \end{bmatrix} \begin{bmatrix} N_1 \\ N_2 \\ N_3 \\ N_4 \end{bmatrix} + \begin{bmatrix} Q \\ 0 \\ 0 \\ 0 \end{bmatrix}$$

or symbolically:

$$\dot{\underset{\sim}{N}}(t) = \underset{\sim}{A}(t)\underset{\sim}{N}(t) + \underset{\sim}{Q}(t) \tag{28}$$

where $\underset{\sim}{A}$ is the transfer matrix between successive time steps. The method can be applied to a general problem in which all the transit times suffer harmonic variations throughout the 24 h.

In order to respect relation (11) the phase of the time T_4 follows that of N_4 and can be estimated from an analysis of the filtering system, while the amplitude can only be adjusted by direct measurement of transit times or N_4 response.

Examples

In order to illustrate the possibilities of the method, several examples were run. The first one corresponds to the data proposed by Izquierdo and Gibbs,[16] the classical reference. *Table 3* presents the data necessary to perform the experiments.

Figure 3(a) represents the S evolution as measured and which has been taken as the origin of the computations. G_2 is a curve predicted according to the constant transit time model. There are no data to compare those predictions. M, however, is the mitotic phase curve whose prediction can be compared to the actual measured data.

Figure 3(b) shows a magnified view of those curves where it is seen that the agreement is promising. Finally, *Figure 3(c)* has been obtained by the step-by-step method when T_4 varies according to *Figure 2*. There is now good agreement, except for the peaks at 10, 12, 14 and 16 h which correspond to the sudden changes in T_4. Taking into account the simplicity of the model, the accuracy obtained is striking.

The second example, *Table 4*, was the treatment of the data proposed by Clausen *et al.*[19] Its interest hinges on the possibility of comparing data for G_2 and M curves in addition to the S curve that is taken as the basis. The mean times are:

$$\bar{T}_1 = 40.39\,\text{h} \qquad \bar{T}_2 = 9.02\,\text{h}$$
$$\bar{T}_3 = 3.21\,\text{h} \qquad \bar{T}_4 = 0.98\,\text{h}$$

Figure 4(a) presents the results obtained while taking:

$$T_4 = 0.98 + \tfrac{1}{2}\sin\frac{2\omega}{24}(t + 12)$$

and maintaining the other transient times as constant. The agreement is again very good for the M curve, except for points around 18 h that, following the hint given in the previous example, can be attributed to sudden changes in T_4.

The agreement in G_2 can be improved by again assuming a variation of the type:

$$T_3 = 3.21 + 0.10\left(\sin\frac{2\omega}{24}(t + 12)\right)$$

As *Figure 4(b)* shows, this has almost no effect on M, and G_2 is lightly displaced to the right but the general trend is the same. Similar results can be obtained by experimenting with other phases and amplitudes. *Figure 4(c)* shows that the results agree very well with those expected from such a model.

Finally, the third example shows the agreement of the model with the authors' own data from the fish *Carassius auratus*. The results obtained from the constant time model are shown in *Figure 1*. It was then decided to use the step-by-step method to model the same case. As shown in *Figure 5(a)*, the results are the same as those of *Figure 1(c)* in spite of the different data treatment.

It was decided to define T as:

$$T_4 = 0.77 + A\sin\frac{2\omega}{24}t$$

where the phase shift was chosen according to the general trends of the response and A was varied in order to get the best possible agreement with the data. As can be seen in *Figure 5(b)*, a value of $A = 0.5$ produces a very good agreement in phase but not in amplitude.

In contrast, when $A = 1$ the compatibility between the prediction and the constant plus fundamental terms of the Fourier development of measured values is almost total, except for the negative values not allowed in the step-by-step procedure. *Figure 5(c)* presents the same solution when $A = 0.98$.

In this example, it seems that for some instants near 16.0 h the transit time is almost zero, producing an infinite flux that momentarily reduces the number of cells in mitosis. The amplitude of T_4 can then be predicted by looking at the minimum values of the M phase. Once again, the discrepancy around 5.0 h can be explained by sudden changes in T_4.

Conclusions

The measurements collected in reference 19 and the comparative examples described in references 29 and 30 show that a deterministic continuous model is, still, a useful approach for interpreting cell cycle evolution.

The numerical results suggest a circadian behaviour, not only for the number of cells but also for the transit time in the mitotic phase.

The simplest approach to reduce the discrepancies is to assume a harmonic evolution of the mitotic transit time, whose amplitude can be adjusted through the minimum of computed values, while the phase is induced thanks to a harmonic analysis or the general trend of the curve.

In all cases there are times at which the transit time suffers severe changes that are immediately reflected in the number of stored cells. In addition, for the case of the fish, *carassius auratus*, there are times with almost zero transit time that are reflected in an emptyness of the M compartment.

All results were obtained on an HP-9836 microcomputer.

Acknowledgements

The authors would like to thank Mrs R. M. Corot for valuable assistance with the histological aspects.

References

1 **Quastler, H. and Sherman, F.G.** Cell population kinetics in the intestinal epithelium of the mouse. *Exp. Cell Res., 1959,* **17,** *420–438*

2 **Kember, N.F., Quastler, H. and Wimber, D.R.** Adaptation of the rat intestine to continuous irradiation. *Brit. J. Radiol., 1962,* **35,** *290*

3 **Cairnie, A.B., Lamerton, L.F. and Steel, G.G.** Cell proliferation studies in the intestinal epithelium of the rat: I: determination of the kinetic parameters. *Exp. Cell Res., 1965,* **39,** *528–538*

4 **Cairnie, A.B., Lamerton, L.F. and Steel, G.G.** Cell proliferation studies in the intestinal epithelium of the rat: II: theoretical aspects. *Exp. Cell Res., 1965,* **39,** *539–553*

5 **Schultze, B.V., Schmeer, A.C. and Maurer, W.** Autoradiographic investigation on the cell kinetics of crypt epithelia in the jejunum of the mouse. Confirmation of steady state growth with constant frequency distribution of cells through the cycle. *Cell Tissue Kinet., 1972,* **5,** *131–145*

6 **Burholt, D.R., Schultze, B. and Maurer, W.** Autoradiographic confirmation of the mitotic division of every mouse jejunal crypt cell labelled with ^{3}H-thymidine. Evidence against the existence of cells synthesizing metabolic DNA. *Cell Tissue Kinet., 1973,* **6,** *229–237*

7 **Scheving, L.E., Burns, E.R., Pauly, J.E. and Tsai, T.H.** Circadian variations in cell division of the mouse alimentary tract, bone marrow and corneal epithelium. *Anat. Rec., 1978,* **191,** *479–486*

8 **Burns, E.R., Scheving, L.E. and Tsai, T.H.** Circadian rhythms in DNA synthesis and mitosis in normal mice and in mice bearing the Lewis lung carcinoma. *Europ. J. Cancer, 1979,* **15,** *233–242*

9 **Neal, J.V. and Potten, C.S.** Circadian rhythms in the epithelial cells of the pericryptal fibroblast shear in three different sites in the murine intestinal tract. *Cells Tissue Kinet., 1981,* **14,** *581–587*

10 **Moller, U. and Larsen, J.K.** The circadian variations in the epidermal growth of the hamster cheek pouch. Quantitative analysis of DNA distributions. *Cell Tissue Kinet., 1978,* **11,** *405–413*

11 **Pilgrim, G., Erb, W. and Maurer, W.** Diurnal fluctuations in the number of DNA synthesizing nuclei in various mouse tissues. *Nature (Lond.), 1963,* **199,** *863*

12 **Sigdestad, C.P., Bauman, J. and Lesher, S.** Diurnal fluctuations in the number of cells in mitosis and DNA synthesis in the jejunum of the mouse. *Exp. Cell Res., 1969,* **58,** *159–162*

13 **Sigdestad, C.P. and Lesher, S.** Further studies on the circadian rhythm in the proliferative activity of mouse intestinal epithelium. *Experientia, 1970,* **26,** *1321–1322*

14 **Potten, C.S., Al-Barwari, S.E., Hume, W.J. and Searle, J.** Circadian rhythms of presumptive stem cells in three different epithelia of the mouse. *Cell Tissue Kinet., 1977,* **10,** *557–568*

15 **Hegazy, M.A.H. and Fowler, J.F.** Cell population kinetics of plucked and unplucked mouse skin: I: unirradiated skin. *Cell Tissue Kinet., 1973,* **6,** *17–33*

16 **Izquierdo, J.N. and Gibbs, S.J.** Circadian rhythms of DNA synthesis and mitotic activity in hamster cheek pouch epithelium. *Exp. Cell Res., 1972,* **71,** *402–408*

17 **Izquierdo, J.N. and Gibbs, S.J.** Turnover of cell-renewing populations undergoing circadian rhythms in cell proliferation. *Cell Tissue Kinet., 1974,* **7,** *99–111*

18 **Brown, J.M. and Berry, R.J.** Relationship between diurnal variation of the number of cells in mitosis and the number of cells synthesizing DNA in the epithelium of the hamster cheek pouch. *Cell Tissue Kinet., 1968,* **1,** *23–33*

19 **Clausen, D.P., Thorud, E., Bjerknes, R. and Elgjo, K.** Circadian rhythms in mouse epidermal basal cells proliferation. Variation in compartment size, flux and phase duration. *Cell Tissue Kinet., 1972,* **12,** *319–337*

20 **Sternfeld Mata, E.** Estudo cinético del ciclo circadiano en células cepa intestinales del pez C auraturs (L), aclimatado a 25°C. *Tésis Doctoral, Univ. Complutense, Madrid, 1982*

21 **Cerrolaza, M^a., Maganto, G. and Nieto, M.** Influencia de la temperatura de aclimatación en la actividad proliferativa del epitelio intestinal del pez C auratus (L). El Sistema Integrado del Ebro: Cuenca, Delta y Medio Marino. *Estudio multidisciplinar. Sem. Com. Conjunto Hisp.-Am. y. Com. Cooperación Cient. y Técnica, Barcelona, 1983*

22 **Al-Dewachi, H.S., Wright, N.A., Appleton, D.R. and Watson, A.J.** Studies on the mechanism of diurnal variation of proliferation indices in the small bowel mucosa of the rat. *Cell Tissue Kinet., 1976,* **9,** *459–467*

23 **Tvermyr, E.F.M.** Circadian rhythms in epidermal mitotic activity. Diurnal variations of the mitotic index, the mitotic rate and the mitotic duration. *Wirchows Arch. B. Cell Path., 1968,* **2,** *318–325*

24 **Maurer, W., Schultze, B., Schmeer, A.C. and Haack, V.** Autoradiographic studies on the mode of growth in the jejunal crypt cells of the mouse. *J. Microsc., 1972,* **96,** *181*

25 **Burns, E.R. and Scheving, L.E.** Circadian influence on the wave of the frequency of labelled mitosis in corneal epithelium. *Cell Tissue Kinet., 1975,* **8,** *61–66*

26 **Moller, U., Jorgen, K. and Faber, M.** The influence of injected tritiated thymidine on the mitotic circadian rhythm in the epithelium of the hamster cheek pouch. *Cell Tissue Kinet., 1974,* **7,** *231–239*

27 **Tvermyr, E.F.M.** Circadian rhythms in hairless mouse epidermal DNA-synthesis as measured by double labelling with ^{3}H-thymidine (^{3}H-Tdr). *Wirchows Arch. B. Cell Path., 1972,* **11,** *43–54*

28 **Hopper, J.L. and Brockwell, P.J.** A stochastic model for cell populations with circadian rhythms. *Cell Tissue Kinet., 1978,* **11,** *205*

29 **Valleron, A.J. and McDonald, P.D.M. (eds.)** Biomathematics and cell kinetics: Developments in cell biology. Vol. 2. *Elsevier/North-Holland, Amsterdam, 1978, 191*

30 **Aarnaes, E., Thorud, E. and Clausen, O.P.** Model analysis of circadian rhythms in mouse epidermal basal cell proliferation. *J. Theor. Biol., 1981,* **88,** *355–370*